



Pergamon

# Discovery of Potent Imidazole and Cyanophenyl Containing Farnesyltransferase Inhibitors with Improved Oral Bioavailability

Yunsong Tong,\* Nan-Horng Lin, Le Wang, Lisa Hasvold, Weibo Wang, Nicholas Leonard, Tongmei Li, Qun Li, Jerry Cohen, Wen-Zhen Gu, Haiying Zhang, Vincent Stoll, Joy Bauch, Kennan Marsh, Saul H. Rosenberg and Hing L. Sham

R47B, AP10, Global Pharmaceutical R&D, Abbott Laboratories, 100 Abbott Park Road, Abbott Park, IL 60064-6101, USA

Received 21 November 2002; accepted 4 February 2003

**Abstract**—A pyridyl moiety was introduced into a previously developed series of farnesyltransferase inhibitors containing imidazole and cyanophenyl (such as **4**), resulting in potent inhibitors with improved pharmacokinetics.

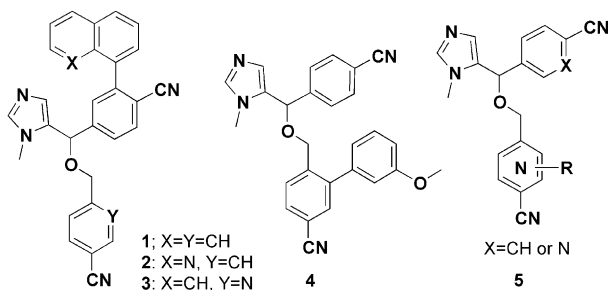
© 2003 Elsevier Science Ltd. All rights reserved.

Ras proteins play an important role in cell growth and oncogenesis.<sup>1</sup> The first step of Ras processing requires transferring a 15-carbon farnesyl group to the C terminal of the protein substrate and is catalyzed by farnesyltransferase (FTase).<sup>2</sup> Inhibitors of FTase prevent the key step in the post-translational processing of the Ras protein. They were developed initially as therapeutic agents to inhibit cell signaling in Ras-transformed cells and thus control the oncogenic Ras activity.<sup>3</sup> Even though it is still debatable whether FTase inhibitors (FTIs) function via Ras blocking,<sup>4</sup> many FTIs show activity in a wide range of preclinical models as well as efficacy in some early clinical trials.<sup>5</sup> Geranylgeranyltransferase-I (GGTase-I), which is closely related to FTase, transfers a 20-carbon group to the C terminal of Ras protein. A recent observation demonstrated that an optimal FTI should be selective for FTase over GGTase to achieve lower toxicity.<sup>6</sup>

During the early studies in search of FTIs, we and others<sup>7</sup> found molecules with imidazole and cyanophenyl moieties, such as **1**, to be potent against FTase. Insertion of nitrogen into the ring system of **1** resulted in compounds **2** and **3** (Table 1) with improved cellular Ras processing (RP) activity as well as acceptable pharmacokinetics (PK).<sup>8</sup> We also found that elimination of the fused rings from molecules like **1**, along with addition of an aromatic ring at the lower cyanophenyl moiety, led to another series of potent and more selective FTIs represented by **4** (Table 1).<sup>8</sup> However, compound **4** possesses relatively low oral bioavailability. In an effort to optimize **4**, we developed molecules containing an additional ring nitrogen (general structure **5**), resulting in FTIs with better PK profiles while maintaining high potency and selectivity.

The chemistry of the nitrogen insertion into the lower cyanophenyl moiety is shown in Scheme 1. 1-Methyl-2-triethylsilylimidazole<sup>9</sup> was treated with *t*-BuLi followed by 4-cyanobenzaldehyde to give the key racemic intermediate **6**. The ether formation was achieved by the reaction of **6** with various benzyl bromides using Ag<sub>2</sub>O. Alternatively, it could be carried out by the coupling of **6** and alcohol **9** using TsOH. The final compounds for the SAR study were synthesized with either direct aminations or Suzuki coupling reactions.

The syntheses of the three key intermediates, **9**, **12**, and **15**, are outlined in Scheme 2. Pyridinone **7** was brominated, then coupled with 3-chlorophenylboronic acid to afford **8**. Sequential treatment of **8** with POCl<sub>3</sub> followed by benzylic bromination and hydrolysis gave compound



\*Corresponding author. Tel.: +1-847-935-1252; fax: +1-847-935-5165; e-mail: yunsong.tong@abbott.com

**Table 1.** Activity and PK comparison of compounds **1–4**

Compd	FTase IC <sub>50</sub> <sup>a</sup> (nM)	GGTase-I IC <sub>50</sub> <sup>b</sup> (nM)	RP EC <sub>50</sub> <sup>c</sup> (nM)	Dog PK <sup>d</sup> F (%) <sup>e</sup>	Monkey PK <sup>d</sup> F (%) <sup>e</sup>
<b>1</b>	0.20	18	110	29	65
<b>2</b>	2.0	103	3.7	53	92
<b>3</b>	0.43	24	6.0	56	48
<b>4</b>	0.62	3900	1.2	35	2.3

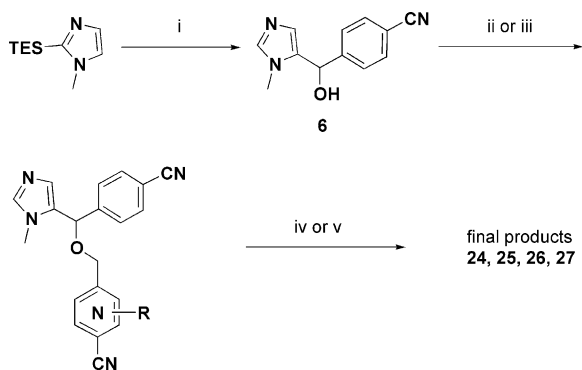
<sup>a</sup>Compound concentration needed to cause 50% inhibition of transfer of [<sup>3</sup>H]FPP to biotin K-ras peptide (KKSKTKCVIM) catalyzed by bovine FTase.

<sup>b</sup>Compound concentration needed to cause 50% inhibition of transfer of [<sup>3</sup>H]FPP to biotin K-ras peptide (KKSKTKCVLL) catalyzed by bovine GGTase-I.

<sup>c</sup>Compound concentration needed to reduce 50% of farnesylation in NIH-3T3 H-ras cell line.

<sup>d</sup>5 mg/kg single dose.

<sup>e</sup>Oral bioavailability.

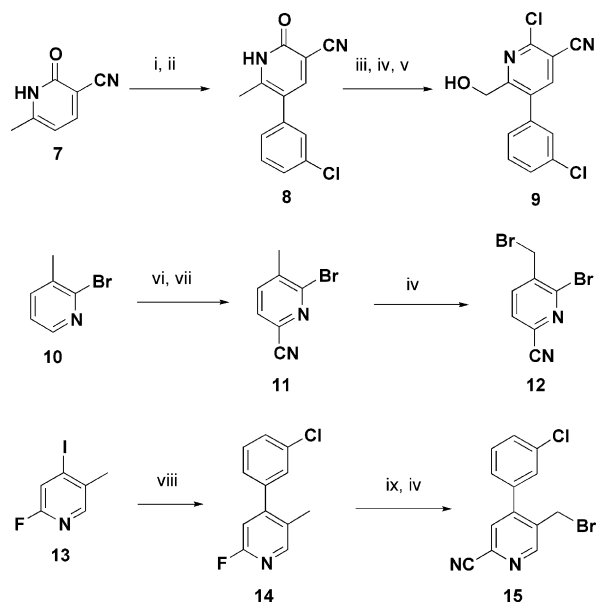


**Scheme 1.** Reagents and conditions: (i) *t*-BuLi, 4-cyanobenzaldehyde, THF,  $-78^{\circ}\text{C}$ , 79%; (ii) **12**, **15**, or 6-bromomethyl-2-chloro-nicotinonitrile, Ag<sub>2</sub>O, CH<sub>2</sub>Cl<sub>2</sub>, rt, 22–50%; (iii) **9**, TsOH, toluene, Dean–Stark trap, reflux, 44%; (iv) amines, heating; (v) ArB(OH)<sub>2</sub>, Pd(PPh<sub>3</sub>)<sub>4</sub>, 2 N Na<sub>2</sub>CO<sub>3</sub>, toluene, EtOH, heating.

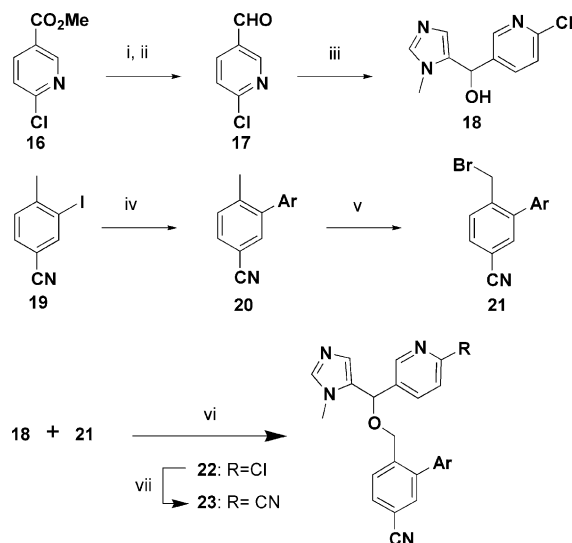
**9.** 2-Bromo-3-methylpyridine **10** was converted into the *N*-oxide using mCPBA, which, in turn was treated with dimethylcarbonyl chloride and TMSCN to afford cyano compound **11**. Benzylic bromination led to bromide **12**. Suzuki coupling of 2-fluoro-4-iodo-5-methylpyridine<sup>10</sup> **13** with 3-chlorophenylboronic acid gave the biaryl molecule **14**. The fluoro group of **14** was converted into a cyano upon treatment with NaCN. Standard bromination gave intermediate **15**.

The compounds with the nitrogen insertion in the upper cyanophenyl moiety were prepared using the chemistry shown in **Scheme 3**. The methylester of **16** was reduced to the alcohol with LAH followed by oxidation with PCC to give aldehyde **17**. Treatment of **17** with 5-lithio-1-methyl-2-triethylsilylimidazole afforded **18**. Molecule **21** was derived from a Suzuki coupling of **19** followed by benzylic bromination of **20**. Compounds **18** and **21** were then coupled via the ether formation described earlier to give **22**. Cyanation of **22** led to the final product **23**.

The FTIs synthesized were evaluated for their biological activities. As shown in **Table 2**, when nitrogen is inserted into the upper cyanophenyl group, the inhibitors (**23**) are as potent as **4** against FTase while maintaining



**Scheme 2.** Reagents and conditions: (i) NBS, dichloroethane, reflux, 92%; (ii) 3-chlorophenylboronic acid, Pd(PPh<sub>3</sub>)<sub>4</sub>, 2 N Na<sub>2</sub>CO<sub>3</sub>, LiCl, toluene, EtOH, 100 °C, 73%; (iii) POCl<sub>3</sub>, 85 °C, 90%; (iv) NBS, CCl<sub>4</sub>, AIBN, reflux; (v) Celite<sup>®</sup>, 1,4-dioxane, H<sub>2</sub>O, reflux, 20%; (vi) mCPBA, CH<sub>2</sub>Cl<sub>2</sub>, rt, 47%; (vii) dimethylcarbonyl chloride, TMSCN, dichloroethane, reflux, 31%; (viii) 3-chlorophenylboronic acid, Pd(PPh<sub>3</sub>)<sub>4</sub>, Na<sub>2</sub>CO<sub>3</sub>, toluene, EtOH, H<sub>2</sub>O, reflux, 80%; (ix) NaCN, DMSO, 110 °C, 90%.



**Scheme 3.** Reagents and conditions: (i) LAH, THF, 44%; (ii) PCC, CH<sub>2</sub>Cl<sub>2</sub>, 78%; (iii) *t*-BuLi, 1-methyl-2-triethylsilylimidazole, THF,  $-78^{\circ}\text{C}$ , 80%; (iv) ArB(OH)<sub>2</sub>, Pd(PPh<sub>3</sub>)<sub>4</sub>, Na<sub>2</sub>CO<sub>3</sub>, toluene, H<sub>2</sub>O, 90 °C; (v) NBS, CCl<sub>4</sub>, AIBN, 50%; (vi) Ag<sub>2</sub>O, CH<sub>2</sub>Cl<sub>2</sub>, 50%; (vii) Zn(CN)<sub>2</sub>, Pd(PPh<sub>3</sub>)<sub>4</sub>, DMF, 190 °C, sealed tube, 40%.

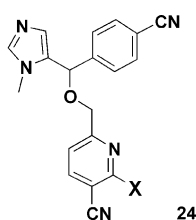
high selectivity over GGTase. Three analogues (**23a**, **23d**, and **23g**) possess EC<sub>50</sub> values less than 10 nM in RP. Compound **23a** has relatively low oral bioavailability (*F* = 9.4%) in monkey (1 mg/kg dosage).

Compounds **24** with substituents *ortho* to the lower cyano group are generally less potent against FTase as compared to **4** (**Table 3**). X-ray structures suggest that these substituents may be too close to the protein residues in the active site.

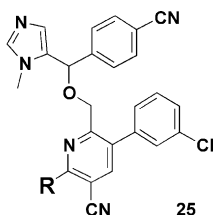
**Table 2.** SAR of pyridyl compounds **23**

Compd	Ar	FTase IC <sub>50</sub> (nM)	GGTase-I IC <sub>50</sub> (nM)	RP EC <sub>50</sub> (nM)
<b>4</b>		0.62	3900	1.2
<b>23a</b>	3-Cl-Ph	0.75	8620	2.1
<b>23b</b>	3-OMe-Ph	0.88	> 10,000	20
<b>23c</b>	3-OCF <sub>3</sub> -Ph	0.40	990	24
<b>23d</b>	3,4-OCH <sub>2</sub> O-Ph	0.84	> 10,000	3.5
<b>23e</b>	3-Cl-4-F-Ph	1.0	8600	46
<b>23f</b>	3,5-di-F-Ph	2.0	> 10,000	25
<b>23g</b>	3,5-di-Cl-Ph	0.64	960	3.5
<b>23h</b>	1-Naphthyl	1.7	> 10,000	46

The results of the SAR studies on series **25** are shown in Table 4. All the compounds are potent against FTase and selective over GGTase. Among them, many have RP EC<sub>50</sub> values below 10 nM. Compound **25d**, with a 4-acyl-piperazine, is three fold more potent than **4** in the cellular RP assay, but does not result in improved oral

**Table 3.** SAR of pyridyl compounds **24**

Compd	X	FTase IC <sub>50</sub> (nM)	GGTase-I IC <sub>50</sub> (nM)
<b>4</b>		0.62	3900
<b>24a</b>	3-Cl-Ph	12	1100
<b>24b</b>	4-Methyl-piperazin-1-yl	58	—
<b>24c</b>	2-Naphthyl	8.2	2600
<b>24d</b>	3,5-di-Cl-Ph	8.5	1600
<b>24e</b>	4-Cl-Ph	25	3900
<b>24f</b>	3-Cyano-Ph	68	—

**Table 4.** SAR of pyridyl compounds **25**

Compds	R	FTase IC <sub>50</sub> (nM)	GGTase-I IC <sub>50</sub> (nM)	RP EC <sub>50</sub> (nM)	PK <sup>a</sup> F (%)
<b>4</b>		0.62	3900	1.2	35 <sup>b</sup>
<b>25a</b>	H	0.92	4200	10	78 <sup>b</sup> , 0.9 <sup>c</sup>
<b>25b</b>	Cl	0.90	2800	29	14 <sup>b</sup>
<b>25c</b>	4-Boc-piperazin-1-yl	0.99	650	4.5	2.6 <sup>b</sup>
<b>25d</b>	4-Acyl-piperazin-1-yl	0.98	2100	0.40	12 <sup>b</sup>
<b>25e</b>	4-Methyl-piperazin-1-yl	0.57	2400	2.0	—
<b>25f</b>	4-Hydroxy-piperidin-1-yl	0.51	830	3.6	14 <sup>b</sup>
<b>25g</b>	4-Carboxamoyl-piperidin-1-yl	0.73	2100	1.5	1.5 <sup>c</sup>
<b>25h</b>	Morpholin-4-yl	0.25	1800	1.2	—

<sup>a</sup>5 mg/kg single dose.

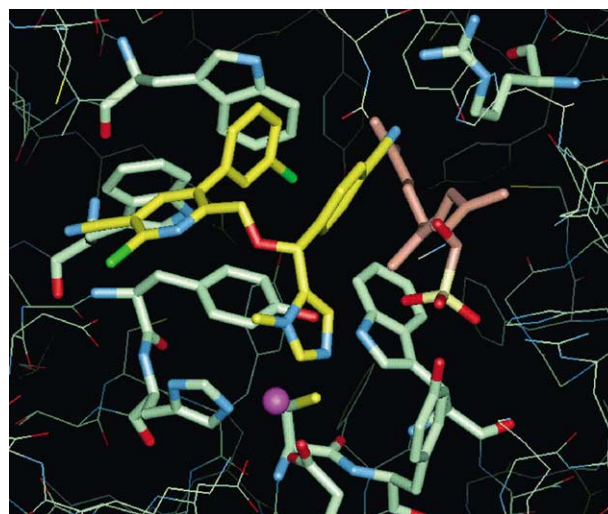
<sup>b</sup>Dog PK.

<sup>c</sup>Monkey PK.

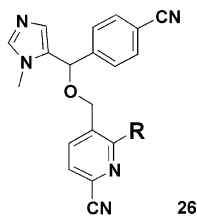
bioavailability in dog. Compound **25a**, which has no substitution at R, shows reasonable PK in dog ( $F=78\%$ ), but fails to perform well in monkey ( $F=0.9\%$ ). A representative X-ray crystallographic structure with compound **25b** bound to the active site of FTase and hydroxyl farnesyl phosphate (HFP)<sup>11</sup> is shown in Figure 1. The nitrogen in the imidazole moiety is ligated to the zinc ion with a distance of 2.6 Angstrom, a hallmark feature of the imidazole-bearing FTIs. The lower cyanophenyl and its 3-chlorophenyl substituent are close to the hydrophobic residues of FTase. The chloro on the pyridyl ring points to the solvent front, which explains why bulky solubilizing replacements of it (**25c** to **25h**) do not sacrifice the potency of the inhibitors. The upper cyanophenyl sits between the hydrophobic residues and the HFP isoprenoid.

Substitutions on the cyanopyridine **26** led to another series of potent and selective FTIs (Table 5). The bicyclic substitution (**26j**) is as active as monocyclic analogues. As compared to **26b**, compound **27**, which has the 3-chlorophenyl substitution on the other side of the pyridine nitrogen, is about 10-fold less active in Ras processing. Several of the most promising compounds were tested for their PK profiles. Among them, compound **26d** exhibits excellent oral bioavailability ( $F=90\%$  in dog, 56% in monkey).

In summary, we have synthesized four series of imidazole-bearing FTIs with nitrogen inserted into one of the cyanophenyl moieties. Most of the inhibitors in series **23**, **25**, and **26** show IC<sub>50</sub> values against FTase less than 1 nM and cellular Ras processing EC<sub>50</sub> values less than 10 nM. In general, these compounds are at least 2000-fold selective over GGTase-I. Compound **26d** exhibits desirable oral bioavailability in dog and monkey, a feature we targeted for improvement from the initial lead molecule **4**. Thus, the nitrogen insertion into the cyanophenyl core of **4** represents an effective way to develop FTIs with balanced properties.



**Figure 1.**<sup>12</sup> X-ray structure of FTI (**25b** active enantiomer) bound to active site. **25b** is colored yellow. Zn ion is purple. Several key FTase residues are green. The isoprenoid group of HFP is shown in brown.

Table 5. SAR of pyridyl compounds **26**

Compd	R	FTase IC <sub>50</sub> (nM)	GGTase-I IC <sub>50</sub> (nM)	RP EC <sub>50</sub> (nM)	PK <sup>a</sup> F (%)
<b>26a</b>		3.9	>10,000	19	—
<b>26b</b>		0.82	1700	1.8	—
<b>26c</b>		0.18	510	2.0	73 <sup>b</sup>
<b>26d</b>		0.18	1100	1.2	90 <sup>b,d</sup> , 56 <sup>c</sup>
<b>26e</b>		0.51	1200	4.0	—
<b>26f</b>		0.71	4800	2.2	93 <sup>b</sup> , 19 <sup>c</sup>
<b>26g</b>		0.45	1400	6.0	—
<b>26h</b>		44	42	—	—
<b>26i</b>		1.9	>10,000	88	—
<b>26j</b>		0.16	5500	7.4	—
<b>27<sup>c</sup></b>		1.8	>10,000	17	—

<sup>a</sup>1 mg/kg single dose.<sup>b</sup>Dog PK.<sup>c</sup>Monkey PK.<sup>d</sup>Other oral PK data:  $t_{1/2}$  = 7.6 h;  $C_{\max}$  = 0.26 mcg/mL;  $T_{\max}$  = 1.0 h; AUC = 2.8 mcg.h/mL.<sup>e</sup>Synthesized from the reaction of **6** and **15**.

## Acknowledgements

X-ray crystallographic data were collected at beamline 17-ID in the facilities of the Industrial Macromolecular Crystallography Association Collaborative Access Team (IMCA-CAT) at the Advanced Photon Source. These facilities are supported by the companies of the Industrial Macromolecular Crystallography Association through a contract with Illinois Institute of Technology (IIT), executed through IIT's Center for Synchrotron Radiation Research and Instrumentation. Use of the Advanced Photon Source was supported by the US Department of Energy, Basic Energy Sciences, Office of Science, under Contract No. W-31-109-Eng-38.

## References and Notes

- (a) Hunter, T. *Cell* **1997**, *88*, 333. (b) McCormick, F. *Nature* **1993**, *363*, 15. (c) Barbacid, M. *Annu. Rev. Biochem.* **1987**, *56*, 779.
- Reiss, Y.; Goldstein, J. L.; Seabra, M. C.; Casey, P. J.; Brown, M. S. *Cell* **1990**, *62*, 81.
- (a) End, D. W. *Invest. New Drugs* **1999**, *17*, 241. (b) Williams, T. M.; Dinsmore, C. J. *Adv. Med. Chem.* **1999**, *4*, 273. (c) Rowinsky, E. K.; Windle, J. J.; Von Hoff, D. D. *J. Clin. Oncol.* **1999**, *17*, 3631. (d) Qian, Y.; Sebti, S. M.; Hamilton, A. D. *Biopoly.* **1997**, *43*, 25.
- (a) Prendergast, G. C. *Curr. Opin. Cell Biol.* **2000**, *12*, 166. (b) Lebowitz, P. F.; Casey, P. J.; Prendergast, G. C.; Thissen, J. A. *J. Biol. Chem.* **1997**, *272*, 15591.
- (a) Ayral-Kaloustian, S.; Salaski, E. *Curr. Med. Chem.* **2002**, *9*, 1003. (b) Gotlib, J.; Dugan, K.; Katamneni, U.; Sridhar, K.; Wright, A. J.; Thibault, A.; Ryback, M. E.; Greenberg, P. L. *Program/Proceedings, 38th Am. Soc. Clin. Oncol. Annual Meeting*, Orlando, FL, 18–21 May 2002. Am. Soc. Clin. Oncol.: Alexandria, VA, 2002 (Abstract #14, see program document for more references).
- Lobell, R. B.; Omer, C. A.; Abrams, M. T.; Bhimnathwala, H. G.; Brucker, M. J.; Buser, C. A.; Davide, J. P.; deSolms, S. J.; Dinsmore, C. J.; Ellis-Huntchings, M. S.; Kral, A. M.; Liu, D.; Lumma, W. C.; Machotka, S. V.; Rands, E.; Williams, T. M.; Graham, S. L.; Hartman, G. D.; Oliff, A. I.; Heimbrook, D. C.; Kohl, N. F. *Cancer Research* **2001**, *61*, 8758.
- See 5(a) for structures of imidazole-containing FTIs developed by Bristol-Myers Squibb, Merck, and Janssen.
- We will disclose detailed results in different accounts.
- Molina, P.; Fresneda, P. M.; Garcia-Zafra, S. *Tetrahedron Lett.* **1996**, *37*, 9353.
- Rocca, P.; Cochennec, C.; Marsais, F.; Thomas-dit-Dumont, L.; Mallet, M.; Godard, A.; Queguiner, G. *J. Org. Chem.* **1993**, *58*, 7832.
- Farnesyl diphosphate (FPP) was replaced by hydroxyl farnesyl phosphate (HFP) in this study.
- See PDB ID 1NT1 for coordinates.